

Lyapunov exponents of quantum trajectories beyond continuous measurements

I.I. Yusipov¹, O.S. Vershinina¹, S.V. Denisov^{1,2}, S.P. Kuznetsov³, and M.V. Ivanchenko^{1,11}

¹¹ *Department of Applied Mathematics, Lobachevsky University, Nizhny Novgorod, Russia*

² *Department of Theoretical Physics, University of Augsburg, Germany*

³ *Kotelnikovs Institute of Radio-Engineering and Electronics of RAS, Saratov, Russia*

Quantum systems interacting with their environments can exhibit complex non-equilibrium states that are tempting to be interpreted as quantum analogs of chaotic attractors. Yet, despite many attempts, the toolbox for quantifying dissipative quantum chaos remains very limited. In particular, quantum generalizations of Lyapunov exponent, the main quantifier of classical chaos, are established only within the framework of continuous measurements. We propose an alternative generalization which is based on the unraveling of a quantum master equation into an ensemble of so-called 'quantum jump' trajectories. These trajectories are not only a theoretical tool but a part of the experimental reality in the case of quantum optics. We illustrate the idea by using a periodically modulated open quantum dimer and uncover the transition to quantum chaos matched by the period-doubling route in the classical limit.

Hamiltonian chaos, a fascinating product of the sensitivity to initial conditions and topological mixing co-existing in phase spaces of classical nonlinear systems, has been extended to the quantum realm quite early. As a result, a profound understanding of the spectral signatures of Hamiltonian quantum chaos [1–4], as well as extension of the classical Lyapunov exponent to coherent quantum dynamics along with the general issues of quantum–classical chaos correspondence [5–11], have been accomplished.

The progress in experimental quantum physics during the last decade has diverted attention from the Hamiltonian idealization to a more realistic vision motivated by cavity quantum electrodynamics [12], quantum optical systems [13], artificial atoms [14] and polaritonic devices [15]. All these systems are open, i.e., they interact with their environments, and therefore are essentially dissipative [16, 17]. This type of quantum evolution turned out to be no less complex and versatile than its Hamiltonian predecessor; even more, an engineered, tailored dissipation can be used to drive many-body systems towards highly entangled pure states [18] or create new topological phases [19].

There are numerous evidences that non-equilibrium asymptotic states of open quantum systems can lead to structures similar to classical chaotic attractors, f.e., on the Poincaré sections reconstructed by using quantum trajectories or through Husimi distributions (and other projections of quantum states on classical spaces) [20–25]. However, quantification of dissipative quantum chaos is still remaining in its infancy. One of the most recent approaches attempts to match variations in the spectral properties of Lindblad generators or its zero-eigenvalue element (that is a asymptotic density matrix [26, 27]) with transitions between regular and chaotic regimes in the corresponding mean-field models [22, 23, 28, 29]. Still, this approach has to overcome many challenges, from establishing the generality to explaining the origins of the observations made.

A promising alternative is to generalize the concept of

the spectrum of Lyapunov exponents, or, for the start, the notion of the largest exponent, to open quantum systems and thus introduce a quantum analogue of local instability. This program implies unraveling of the solution of the master equation into a set of quantum trajectories and estimating the divergence rate between the close trajectories or, similar to the classical case, performing a time-series analysis for a single trajectory. The only existing realization of this idea is restricted to the framework of continuous measurements, which deals with trajectories of the stochastic Schrödinger equation [30]. This approach allowed to obtain Lyapunov exponents for a quantum version of periodically modulated Duffing oscillator, albeit in the vicinity of the classical limit [31, 32]. It allows (potentially) to go deeper into the quantum regime; however, decreasing value of Lyapunov exponent renders discrimination between regular and chaotic quantum states hard and controversial [34–36].

Despite its successes, the continuous measurement framework is not free from limitations. The main issue is the physical relevance of the corresponding quantum trajectories and thus a possibility to estimate Lyapunov exponents in experiments. This is, in principle, possible but demands quite specific setups [37]. Another issue is a high computational cost of the approach, that constrains numerical studies to the resolution of single-parameter behavior of model systems [32, 33].

In this paper we propose an alternative approach to quantum generalization of Lyapunov exponents. Our approach defines the largest quantum Lyapunov exponent in terms of another unraveling of the master equation, leading to an ensemble of quantum trajectories marked by discrete-time dissipative events called 'quantum jumps' [38–41]. Quantum jump ideology is very relevant in the context of quantum optics and cavity systems [17]. Computational efficiency of the currently available numerical implementation of the quantum jump approach [42] allows us to explore the parameter space of a scalable quantum model and reveal a complex structure of intermingled

regular and chaotic domains. We also go deep into the quantum regime and quantify in there transitions corresponding to the classical period-doubling route to chaos for the first time.

Model.— In the Markovian approximation framework (weak coupling limit to an environment), the evolution of an open quantum system can be described by the Lindblad master equation [16, 27],

$$\dot{\varrho} = \mathcal{L}(\varrho) = -i[H, \varrho] + \mathcal{D}(\varrho), \quad (1)$$

where the first term on the r.h.s. captures the unitary evolution of the system, and the second one describes the action of the environment. We consider a system of N indistinguishable interacting bosons, which hop between sites of a periodically rocked dimer. This model is a popular theoretical testbed [43–45], recently implemented in experiments [46, 47], which is known to exhibit regular and chaotic regimes [22–25]. Its unitary dynamics is governed by a Hamiltonian

$$H(t) = -J \left(b_1^\dagger b_2 + b_2^\dagger b_1 \right) + \frac{2U}{N} \sum_{g=1,2} n_g (n_g - 1) + \varepsilon(t) (n_2 - n_1). \quad (2)$$

Here, J denotes the tunneling amplitude, U is the interaction strength, and $\varepsilon(t)$ presents a periodical modulation of the on-site potentials. In particular, we choose $\varepsilon(t) = \varepsilon(t+T) = \mu_0 + \mu_1 Q(t)$, where μ_0 and μ_1 denote a static and a dynamically varying, respectively, energy offset between the two sites. $Q(t)$ itself is a periodically varying, unbiased two-valued quench-function within one full period T ; more specifically, $Q(\tau) = 1$ within $0 < \tau \leq T/2$ and $Q(\tau) = -1$ for the second half period $T/2 < \tau \leq T$. The boson operators b_g and b_g^\dagger are the annihilation and creation operators on site $g \in \{1, 2\}$, while $n_g = b_g^\dagger b_g$ is the particle number operator. The system Hilbert space has dimension $N+1$ and can be spanned with the N Fock basis vectors, labeled by the number of bosons on the first site n , $\{|n+1\rangle\}$, $n = 0, \dots, N$. Thus, the model size is controlled by the total number of bosons.

The dissipative term involves a single jump operator [18]:

$$\mathcal{D}(\varrho) = \frac{\gamma}{N} \left(V \varrho V^\dagger - \frac{1}{2} \{V^\dagger V, \varrho\} \right), \quad (3)$$

$$V = (b_1^\dagger + b_2^\dagger)(b_1 - b_2), \quad (4)$$

which attempts to “synchronize” the dynamics on the sites by constantly recycling anti-symmetric out-phase modes into symmetric in-phase ones. The dissipative coupling constant γ is taken to be time-independent. Throughout the paper we will assume $J = 1, \mu_0 = 1, \gamma = 0.1$ and $T = 2\pi$.

We employ quantum Monte-Carlo wave function (‘quantum jump’) method to unravel deterministic equation (1)

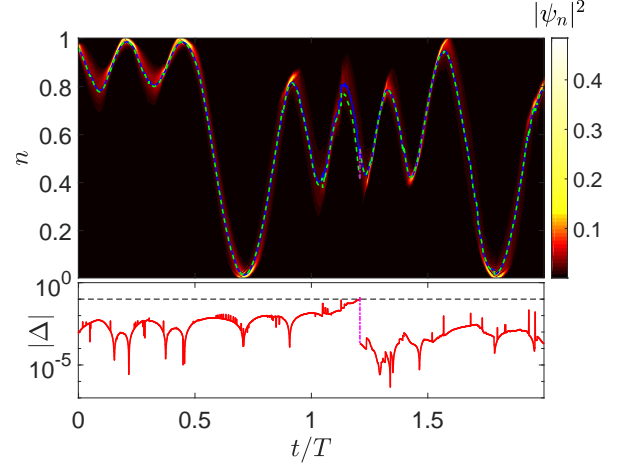


FIG. 1. (Color online) Evolution of fiducial and perturbed trajectories. Top panel: expectations $n_f(t)$ (blue, solid) and $n_a(t)$ (green, dashed), together with fiducial wave function amplitude $|\psi_f(t)|^2$ (color coded). Bottom panel: evolution of the mismatch between the expectations for the two quantum trajectories, $\Delta(t)$. Visible spikes correspond to single quantum jumps, magenta vertical line indicates resetting the perturbed trajectory, when the mismatch overcomes a threshold $\Delta_{max} = 0.1$ (black dashed horizontal line). Here $U = 0.5, \mu_1 = 1.5, N = 200$.

into an ensemble of quantum trajectories [38–41]. It recasts the evolution of the model system in terms of pure states and wave function, $\psi(t)$, governed by an effective non-Hermitian Hamiltonian,

$$\tilde{H} = H - \frac{i}{2} V^\dagger V, \quad (5)$$

and random jumps induced by the dissipator V .

The density matrix can then be sampled from a set of M_r realizations as $\varrho(t_p; M_r) = \frac{1}{M_r} \sum_{j=1}^{M_r} |\psi_j(t_p)\rangle \langle \psi_j(t_p)|$, which, given an initial pure state ψ^{init} for Eq. (5), converges towards the solution of Eq. (1) at time t_p for the initial density matrix $\varrho^{\text{init}} = |\psi^{\text{init}}\rangle \langle \psi^{\text{init}}|$. We make use of a recent high-performance realization of the quantum jumps method [42], generate $M_r = 10^2$ different trajectories for averaging, leave $t_0 = 2 \cdot 10^3 T$ time for relaxation towards an asymptotic state, and follow the dynamics for up to $t = 10^3 T$.

The further analysis is focused on the two observables, that are a normalized number of particles on the left site of the dimer, $n(t)$, and energy expectation, $\epsilon(t)$, that are calculated for each quantum trajectory:

$$n(t) = \frac{1}{N} \sum_k \langle \psi(t) | b_1^\dagger b_1 | \psi(t) \rangle, \quad (6)$$

$$\epsilon(t) = \langle \psi(t) | H | \psi(t) \rangle. \quad (7)$$

The former observable has a phase variable counterpart in the nonlinear mean-field equation for the classical model and will be discussed later.

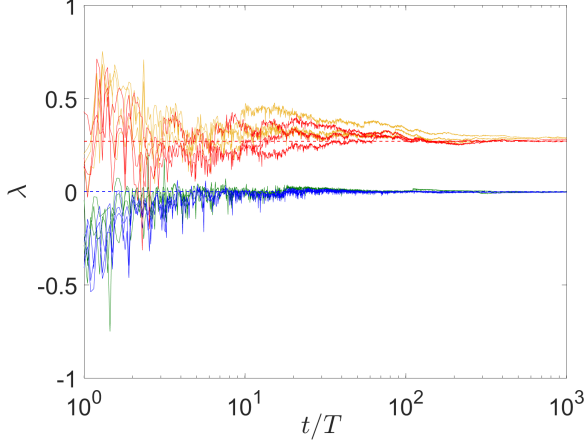


FIG. 2. (Color online) Finite time Lyapunov exponents converging to $\lambda = 0$ (regular) and $\lambda \approx 0.27$ (chaotic regime) for three individual trajectories per case. Based on observable $n(t)$: $U = 0.05$ (blue), $U = 0.5$ (red), and observable $\epsilon(t)$: $U = 0.05$ (green), $U = 0.5$ (yellow). Here $\mu_1 = 1.5$, $N = 200$.

To calculate the largest Lyapunov exponent, we evolve a fiducial and auxiliary trajectories, $\psi_f(t)$ and $\psi_a(t)$, under Eq. (5). The latter trajectory is initialized as a normalized perturbed vector $\psi_a^{init} = \psi_f^{init} + \varepsilon\psi_r$, produced with random i.i.d. entries in ψ_r and $\varepsilon \ll 1$. A representative illustration (see Fig. 1) demonstrates that the wave function $\psi(t)$ remains well-localized during evolution even in an aperiodic regime. The fiducial and perturbed observables, $n_f(t)$ and $n_a(t)$, remain close to each other over many quantum jump events; as their difference $\Delta(t) = |n_f(t) - n_a(t)| > \Delta_{max}$ gets over a threshold, the perturbed state is set back closer to the fiducial one along the mismatch direction $\psi_f(t) - \psi_a(t)$ and normalized. The Lyapunov exponent is routinely estimated following the divergence of a chosen observable as $\lambda(t) = \frac{1}{t} \ln \frac{\Delta(t)}{\Delta(0)}$.

To validate the method we consider two interaction strength values, $U = 0.05$ and $U = 0.5$ (the other parameters are $\mu_1 = 1.5$, $N = 200$), for which regular and chaotic regimes have been previously identified by other means [23] (see also Fig. 3). Lyapunov exponents calculated for individual quantum trajectories demonstrate convergence to asymptotic values, zero and positive for corresponding cases (Fig. 2). Moreover, the result has turned out to be independent on the choice of a particular observable between the two. Further on, we make use of n and average Lyapunov exponents over $M_r = 100$ trajectories.

Next we analyze a transition to dissipative quantum chaos by means of the above described method. First, we introduce the classical counterpart model as a reference. In the limit $N \rightarrow \infty$ the dynamics of quantum dimer can be approximated with mean-field equations for the expectation values of three pseudo-spin opera-

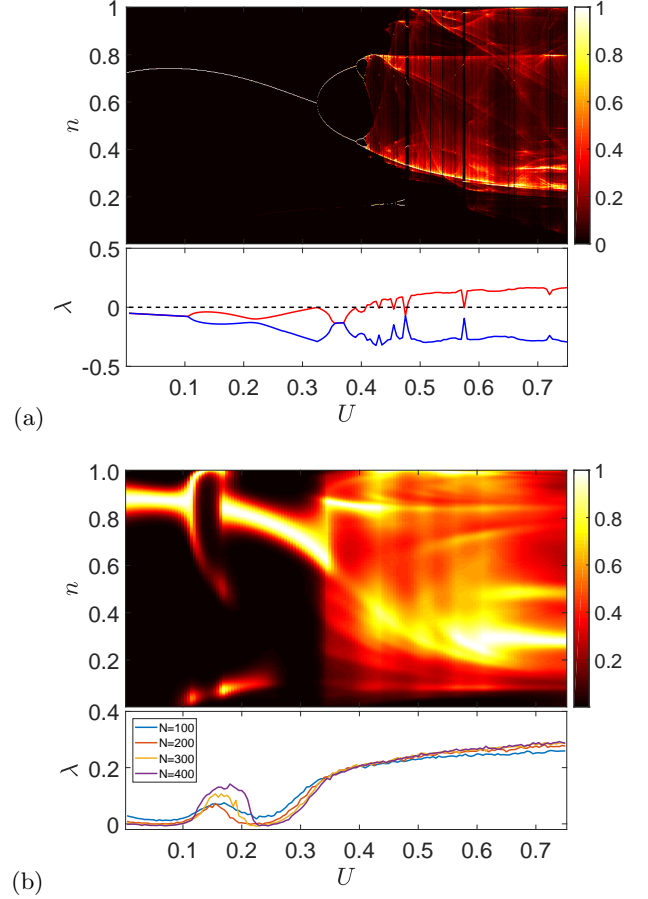


FIG. 3. (Color online) Classical-quantum correspondence in chaos development and Lyapunov spectrum in dependence on interaction strength U . Mean-field model (a) top panel: color-coded histogram for the generated stroboscopic map, bottom panel: Lyapunov spectrum (includes $\lambda = 0$ for a time variable, horizontal dashed line). Quantum model (b) top panel: color-coded probability to observe a fraction of particles n in the asymptotic regime (the maximal element normalized to 1), $N = 200$, bottom panel: quantum largest Lyapunov exponent for different number of particles N . Here $J = 1$, $\mu_0 = 1$, $\mu_1 = 1.5$.

tors $S_x = \frac{1}{2N} (b_1^\dagger b_2 + b_2^\dagger b_1)$, $S_y = -\frac{i}{2N} (b_1^\dagger b_2 - b_2^\dagger b_1)$, $S_z = \frac{1}{2N} (n_1 - n_2)$. For a large number of atoms, the commutator $[S_x, S_y] = [iS_z/N] \xrightarrow{N \rightarrow \infty} 0$ and similarly for other cyclic permutations. Replacing operators with their expectation values, $\langle S_k \rangle = \text{tr}[\varrho S_k]$, and denoting $\langle S_k \rangle$ by S_k , one obtains the semi-classical equations of motion [22]

$$\begin{aligned} \dot{S}_x &= 2\varepsilon(t)S_y - 8US_zS_y + 8\gamma(S_y^2 + S_z^2), \\ \dot{S}_y &= -2\varepsilon(t)S_x + 8US_xS_z + 2JS_z - 8\gamma S_xS_y, \\ \dot{S}_z &= 2JS_y - 8\gamma_0 S_xS_z. \end{aligned} \quad (8)$$

As $S^2 = S_x^2 + S_y^2 + S_z^2 = 1/4$ is a constant of motion, we can reduce the mean-field evolution to the surface of a Bloch

sphere, $(S_x, S_y, S_z) = \frac{1}{2}(\cos \varphi \sin \vartheta, \sin \varphi \sin \vartheta, \cos \vartheta)$, yielding the equations of motion

$$\begin{aligned}\dot{\varphi} &= 2J \frac{\cos \vartheta}{\sin \vartheta} \cos \varphi - 2\varepsilon(t) + 4U \cos \vartheta - 4\gamma \frac{\sin \varphi}{\sin \vartheta}, \\ \dot{\vartheta} &= 2J \sin \varphi + 4\gamma \cos \varphi \cos \vartheta.\end{aligned}\quad (9)$$

A convenient choice to match the quantum and classical solutions is to follow the fraction of particles at the first site, which classical counterpart is $n(t) = [1 + \cos \theta(t)]/2$.

Upon tuning parameter values, the nonlinear mean-field equations display complex dynamics; in particular, period-double route to chaos [22, 23, 25]. Fig. 3 presents a representative diagram by means of the stroboscopic map, $n_k = n(t_0 + kT)$, generated by the flow, Eq.(9), U taken as a bifurcation parameter, and $\mu_1 = 1.5$. One classical Lyapunov exponent becomes positive with emergence of the chaotic attractor, while another is remaining negative, and the one corresponding to the time variable is simply zero.

Depending on parameter values, the interaction with the environment can strongly localize quantum trajectories on the classical ones [20, 21, 31, 32]. Our case is notably different: At any instant of time quantum trajectories are well-localized in the Fock space (Fig. 1), but they do not follow the classical mean-field trajectories, as the resulting structure of the probability distribution for n has only a general structural resemblance, see Fig. 3(b), top. Nevertheless, working in the essentially quantum regime and tuning number of bosons N , we consistently reproduce the emergence of the positive largest quantum Lyapunov exponent following the structural chaotization of the asymptotic solution, see Fig. 3(b).

It is noteworthy that on the interval $U \in [0.1, 0.2]$, where the quantum asymptotic solution undergoes some structural bifurcation, quantum Lyapunov exponent becomes positive while the classical mean-field equations still yield a period-1 limit cycle. Stability analysis of the mean-field dynamics gives a clue about possible resolution of this paradox. Indeed, we find that the largest Lyapunov exponent is approaching and almost touches zero line, Fig. 3(a), bottom, a signature of bifurcation that is nearly avoided in the mean-field approximation, but is full-fledged in the genuine quantum system. Whether the positive quantum Lyapunov exponent reflects a dynamical property of the system, although the structure of the asymptotic solution lacks an apparent structural complexity, or it reflects a particular quantum-specific effect, is the issue which deserves further studies.

Finally, we report the result of an extensive numerical experiment aimed at calculation – for model (1-2) – of the largest quantum Lyapunov exponent as a function of the particle interaction strength and the amplitude of periodic modulations. The dynamics generated by the mean-field equations reveals that chaotic regimes are abundant on the two-parameter plane. The quantum phase diagram,

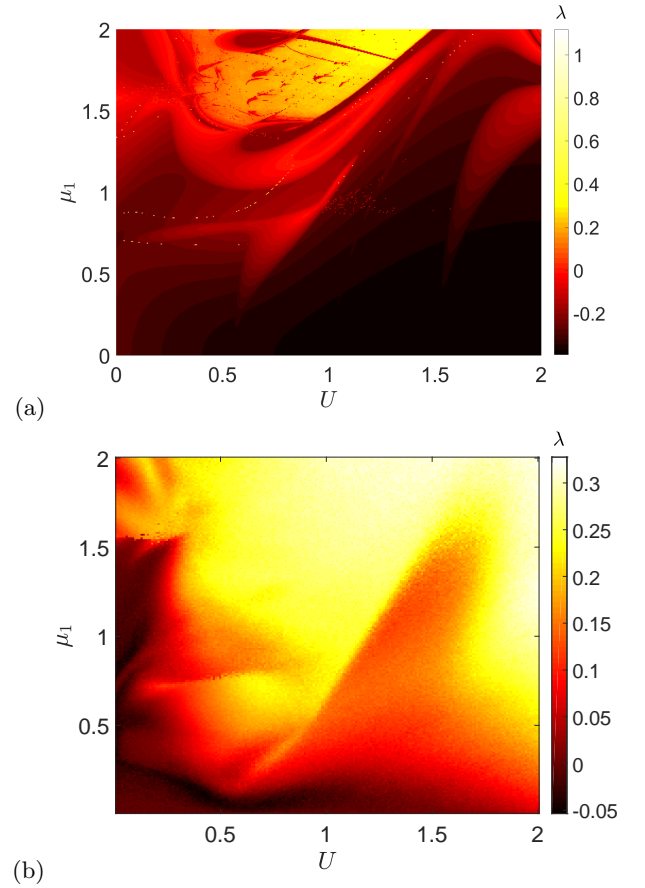


FIG. 4. (Color online) Phase diagram in the interaction – driving amplitude plane for the periodically modulated (a) mean-field and (b) open quantum dimer. The color-coded quantum Lyapunov exponent indicates regular and chaotic regimes. Here $N = 100$.

in general, replicate this; see it Fig. 4. The quantum case, however, exhibits a considerably earlier development of chaos and a more complicated structure of regular and chaotic regions. In particular, it follows that multiple two-way transitions are possible, if one of the parameters is fixed and another increased. It can be explained by the reduced complexity of the mean-field model (9). We conjecture that by going to the higher-order mean-field approximations, by increasing the truncation order of accounted correlation functions, and hence, by increasing the dimension of resulting nonlinear system, we could also observe an expansion of the chaotic area.

In conclusion, we proposed an approach to calculate the largest Lyapunov exponent for open quantum systems based on the quantum jump (Monte-Carlo wave function) unraveling of the Lindblad equation. A numerical realization of this idea allowed us to capture a quantum analogue of the period-doubling route to chaos in a periodically modulated many-body system. The stability analysis helped us to understand the origin of a ‘genuine

quantum’ bifurcation, absent in the corresponding classical mean-field dynamical system. The obtained phase diagram on the parameter plane “interaction strength – amplitude of modulations” revealed a complex structure of regular and chaotic regions with the two-side transitions happening upon the variations of each of the two parameters. Our findings give an new outlook on the dynamics of open quantum systems, especially in such fields as quantum electrodynamics, quantum optics, and polaritonic devices, where the quest for the signatures and quantifiers of dissipative quantum chaos is getting a growing interest.

The authors acknowledge support of Russian Foundation for Basic Research grant No. 17-32-50078 (IY and SK), President of Russian Federation grant No MD-6653.2018.2 (OV and MI), and Ministry of Education and Science of the Russian Federation Research Assignment No. 1.5586.2017/BY (MI). Numerical simulations were carried out at the Lobachevsky University Supercomputer.

-
- [1] G. Casati, B. Chirikov, F. Izraelev, and J. Ford, in *Stochastic Behavior in Classical and Quantum Hamiltonian Systems*, Lect. Notes Phys. Vol. 93, edited by G. Casati and J. Ford (Springer, Berlin, 1979), pp. 334352.
 - [2] M. Gutzwiller, *Chaos in Classical and Quantum Mechanics* (Springer, New York, 1991).
 - [3] F. Haake, *Quantum Signatures of Chaos*, 3rd ed. (Springer-Verlag, Berlin, 2010).
 - [4] T. Guhr, A. Müller-Groeling, and H.A. Weidenmüller, Phys. Rep. **299**, 189 (1998).
 - [5] M. Toda and K. Ikeda, Phys. Lett. A **124**, 165 (1987).
 - [6] F. Haake, H. Wiedemann, and K. Życzkowski, Ann. Phys. (N.Y.) **504**, 531 (1992).
 - [7] I.L. Aleiner and A.I. Larkin, Phys. Rev. E **55**, R1243 (1997).
 - [8] S.P. Kuznetsov, Izvestiya VUZ. Applied Nonlinear Dynamics, 1998, **6**, p.3 (In Russian.)
 - [9] S.P. Kuznetsov, Physica D **137**, 205 (2000).
 - [10] J. Maldacena, S. H. Shenker, and D. Stanford, J. High Energy Phys. **08**, 106 (2016).
 - [11] E.B. Rozenbaum, S. Ganeshan, and V. Galitski, Phys. Rev. Lett. **118**, 086801 (2017).
 - [12] H. Walther, B.T.H. Varcoe, B.-G. Englert, Th. Becker, Rep. Prog. Phys. **69**, 1325 (2006).
 - [13] M. Aspelmeyer, T.J. Kippenberg, F. Marquardt, Rev. Mod. Phys. **86**, 1391 (2014).
 - [14] J.Q. You and F. Nori, Nature **474**, 589 (2011).
 - [15] T. Feurer, J.C. Vaughan, and K.A. Nelson, Science **299**, 374 (2003).
 - [16] Breuer, H.-P. and F. Petruccione, *The Theory of Open Quantum Systems* (Oxford University Press, Oxford, 2002).
 - [17] H.J. Carmichael, *An Open Systems Approach to Quantum Optics* (Springer, Berlin, 1993).
 - [18] S. Diehl, A. Micheli, A. Kantian, B. Kraus, H.P. Büchler, P. Zoller, Nature Phys. **4**, 878 (2008).
 - [19] J.C. Budich, P. Zoller, and S. Diehl, Phys. Rev. A **91**, 042117 (2015).
 - [20] T.P. Spiller, J.F. Ralph, Phys. Lett. A **194**, 235 (1994).
 - [21] T.A. Brun, I.C. Percival, and R. Schack, J. Phys. A: Math. Gen. **29**, 2077 (1996).
 - [22] M. Hartmann, D. Poletti, M. Ivanchenko, S. Denisov, P. Hänggi, New J. Phys. **19**, 083011 (2017).
 - [23] M.V. Ivanchenko, E.A. Kozinov, V.D. Volokitin, A.V. Liniov, I.B. Meyerov, and S.V. Denisov, Ann. Phys. **529**, 1600402 (2017).
 - [24] G.G. Carlo, L. Ermann, A.M.F. Rivas, M.E. Spina, and D. Poletti, Phys. Rev. E **95**, 062202 (2017).
 - [25] R.R.W. Wang, B. Xing, G.G. Carlo, and D. Poletti, Phys. Rev. E **97**, 020202(R) (2018).
 - [26] G. Lindblad, Commun. Math. Phys. **48**, 119 (1976).
 - [27] Alicki, R. and K. Lendi, 1987, *Quantum Dynamical Semigroups and Applications*, Lecture Notes in Physics, Vol. 286 (Springer, Berlin, 1998).
 - [28] R. Grobe, F. Haake, and H.-J. Sommers, Phys. Rev. Lett. **61**, 1899 (1988).
 - [29] T. Prosen and M. Žnidarič, Phys. Rev. Lett. **111**, 124101 (2013).
 - [30] N. Gisin and I.C. Percival, J. Phys. A: Math. Gen. **25**, 5677 (1992).
 - [31] T. Bhattacharya, S. Habib, and K. Jacobs, Phys. Rev. Lett. **85**, 4852 (2000).
 - [32] B. Pokharel, M.Z.R. Misplon, W. Lynn, P. Duggins, K. Hallman, D. Anderson, A. Kapulkin and A.K. Pattanayak, Sci. Rep. **8**, 2108 (2018).
 - [33] S. Habib, K. Jacobs, and K. Shizume, Phys. Rev. Lett. **96**, 010403 (2006).
 - [34] A. Kapulkin and A. Pattanayak, Phys. Rev. Lett. **101**, 074101 (2008).
 - [35] J. Finn, K. Jacobs, and B. Sundaram, Phys. Rev. Lett. **102**, 119401 (2009).
 - [36] K. Kingsbury, C. Amey, A. Kapulkin, and A. Pattanayak, Phys. Rev. Lett. **102** 119402 (2009).
 - [37] H. Wiseman, J. Phys. A **49**, 411002 (2016).
 - [38] R. Dum, A.S. Parkins, P. Zoller, and C.W. Gardiner, Phys. Rev. A **46**, 4382 (1992).
 - [39] K. Mølmer, Y. Castin, and J. Dalibard, J. Opt. Soc. Am. B **10**, 524 (1993).
 - [40] M. B. Plenio and P. L. Knight, Rev. Mod. Phys. **70**, 101 (1998).
 - [41] A.J. Daley, Adv. Phys. **63**, 77 (2014).
 - [42] V. Volokitin, A. Liniov, I. Meyerov, M. Hartmann, M. Ivanchenko, P. Hanggi, and S. Denisov, Phys. Rev. E **96**, 053313 (2017).
 - [43] A. Vardi and J. R. Anglin, Phys. Rev. Lett. **86**, 568 (2001).
 - [44] F. Trimborn, D. Witthaut, and S. Wimberger, J. Phys. B: At. Mol. Opt. Phys. **41**, 171001 (2008).
 - [45] D. Poletti, J.-S. Bernier, A. Georges, and C. Kollath, Phys. Rev. Lett. **109**, 045302 (2012).
 - [46] C. Gross, T. Zibold, E. Nicklas, J. Esteve, and M. K. Oberthaler, Nature **464**, 1165 (2010).
 - [47] J. Tomkovič, W. Muessel, H. Strobel, S. Lööck, P. Schlagheck, R. Ketzmerick, and M. K. Oberthaler, Phys. Rev. A **95**, 011602 (2017).